Flexible White Lighting Fabricated With Quantum Dots Color Conversion Layers Excited by Blue Organic Light-Emitting Diodes

Fuh Shyang Juang, Chong Zhe Jian, Krishn Das Patel, and Hao Xuan Wang

***Abstract*—In this study, HATCN is coated on flexible PET/indium tin oxide (ITO) substrate as a modified layer and a hole injection layer to improve the hole injection from ITO. Then a blue organic light emitting diode (OLED) can successfully be fabricated without a surface treatment procedure (O_2 plasma or UV Ozone treatment). The new blue TADF series fluorescent material is employed as emitting layer with a luminescence wavelength of 456 nm. Also, it has a narrow full width at a half maximum (FWHM) of 26 nm featuring excellent color chromaticity. Quantum dot (QD) photoresist is a perfect color conversion material featuring good color adjustability, narrow emission spectrum, high luminous efficiency, and simple spin-coating processes. In this study, the photoresist mixed with green and red quantum dots is used as a color conversion layer (CCL), and a blue OLED is utilized to excite green and red CCL. To test the material of QD photoresist, it is coated on the substrate of another piece of glass first and then the blue OLED is utilized to remotely excite green and red QD CCL. The fluorescence characteristic of QD photoresist is explored to acquire a spectrum of 528 nm and 620 nm. In the device structure of a blue OLED, the electron-and hole-only current density is compared and the hole transport layer TAPC thickness is adjusted to improve the luminance and efficiency. Finally, green and red quantum dot photoresist is mixed using a proper ratio and then directly coated on the back of the PET/ITO substrate. Furthermore, the thickness of the QD photoresist is adjusted to increase the QD excited fluorescence. The blue OLED and QD CCL was integrated to generate three primary colors, i.e., blue, green, and red. Finally, a flexible white OLED lighting panel is successfully fabricated using simple processes. Moreover, it features high-spectrum stability. The CIE coordinates will not drift with bias, thus, it can resist the voltage variation.**

***Index Terms*—Color conversion layer, flexible, lighting, OLED, TADF, white.**

I. Introduction

WHITE organic light-emitting diodes (WOLED) can be used as general solid state lighting and is light and flexible, thus offering more convenience for everyday life. The structure of flexible blue OLED devices faces two main problems at present: (1) The highest occupied molecular orbital (HOMO) of blue emitting layer (EML) has a very large energy level and high hole-injection barrier between the ITO work function and the HOMO of blue EML, resulting in uneasy hole injection; (2) The surface condition of ITO on flexible substrates is unfavorable with a very high roughness and resistance. Therefore, how to improve the hole injection efficiency between ITO and EML is an important consideration.

The characteristics of OLED is very sensitive to the surface conditions of ITO. The root-mean-square (RMS) value of surface roughness of glass is approximately 2 nm while that of PET is approximately 9 nm. Besides, the adhesive capacity between ITO and flexible PET substrates is not strong enough, and consequently, ITO is very easy to crack. To avoid cracking, the duration of UV ozone treatment on the ITO film of flexible substrate cannot be too long. Therefore, the surface of flexible ITO cannot be deeply cleaned and the surface modification of flexible ITO becomes very important. Some modified layers have already been used to improve ITO work function and improve their surface morphology. For example, the utilization of organic material 1,4,5,8,9,11-hexaazatriphenylene-hexacarbonitrile (HATCN) with an energy level of deep-lying lowest unoccupied molecular orbital (LUMO) (approximately 5.4-5.7 eV) can enhance the hole injection rate from anode. For example, the use of HATCN in ITO/NPB interfaces can inhibit or eliminate NPB crystallization. ITO/HATCN/NPB benefits the hole injection and thus, it can improve the thermal stability of OLED and extend the lifetime of the device [1]. The electron-hole pairs would be generated in the interface of HATCN/NPB. HATCN transmits electrons to ITO while NPB transmits holes to EML. Therefore, the HATCN on ITO can increase the work function of ITO surface and increase the stability in ITO/HATCN interface [2]. MoO_3 can also be inserted between HATCN and NPB (HATCN/MoO_3 (1-5 nm)/NPB), because HATCN/MoO_3 can reduce the accumulation of the space charge between ITO electrodes and NPB layer and reduce exciton quenching to extend the OLED lifetime. After ITO is evaporated with HATCN, the work function of ITO can be increased to approximately 5.2-5.4 eV. Meanwhile, the energy level of the valence band of MoO_3 is approximately 5.5 eV which can ensure a smooth injection and transmission of holes [3], [4]. Therefore, HATCN can be directly evaporated on an untreated PET/ITO surface.

Manuscript received October 6, 2021; revised January 23, 2022; accepted February 3, 2022. Date of publication February 8, 2022; date of current version February 18, 2022. This work was supported in part by the Taiwan Ministry of Science and Technology under Grants MOST-109-2221-E-150-014 and MOST-110-2221-E-150-013. *(Corresponding author: Fuh Shyang Juang.)*

The authors are with the Department of Elecrto-Optical Engineering, National Formosa University, Huwei, Yunlin 63208, Taiwan (e-mail: fsjuang@gs.nfu.edu.tw; 10876112@gm.nfu.edu.tw; d0977108@gm.nfu.edu.tw; 10876116@gm.nfu.edu.tw).

Digital Object Identifier 10.1109/JPHOT.2022.3149385

In other words, it is not required to treat ITO surfaces using O_2 plasma or UV Ozone first, and avoiding damage of the PET/ITO substrate due to excessive cleaning with organic solvent.

Despite the high luminous efficiency, the blue phosphorescence materials of OLED also have certain shortcomings, e.g., the high cost of the heavy metal utilized and the relatively wide FWHM of the luminescence spectrum of blue phosphorescence materials. The full color of OLED and white-lighting illumination will become increasingly perfect with the maturity of blue fluorescent materials. Therefore, a blue material of thermally activated delayed fluorescence (TADF) has become a development highlight in recent years. A TADF new blue material of *N7,N7,N13,N13*,5,9,11,15-octaphenyl-5,9,11,15-tetrahydro-5,9,11,15-tetraaza-19*b*,20*b*-diboradinaphtho [3,2,1-*de*:1′,2′,3′-*jk*]pentacene-7,13-diamine (ν-DABNA) containing no heavy metals, featuring narrow FWHM, and high quantum efficiency has been highly valued [5], [6], [7]. The adoption of the novel blue material is also a feature of this research.

Quantum dot (QD) features a relatively high fluorescent efficiency with wide-gamut range performance. It can be used as color conversion materials. Currently, the OLED mainstream manufacturing technologies employ different red green blue (RGB) emitting layers to be mixed to generate the white light. However, the use of RGB multi-layers or multi-dopant emitting layers presents many problems including the difficult adjustment of the luminous intensity of each emitting layer and the difficulty to accurately control the white-light CIE chromaticity coordinates. Besides this, due to the different lifetimes of each emitting layer, the luminescence spectrum will change with time, further resulting in white-light distortion. To solve these aforementioned shortcomings, blue OLED plus CCL can be adopted. The use of a stable blue OLED and green+red color conversion layers can improve the color stability. Additionally, the processes are relatively easy.

The luminescence wavelength can be adjusted using QD dimensions which also have a high photoluminescence (PL) quantum efficiency. It has a relatively high absorbing rate at blue wavelength which can increase the color conversion efficiency. Thus, QD can be used as a perfect color conversion material [8]. QD material has presented high potential to become the next generation of monitor and lighting due to its advantages, such as its feasibility with solution process, good color adjustability, narrow FWHM, high luminous efficiency, and longer lifetime of QD as an inorganic material than that of organic materials [9].

Maojun Yin, *et al.* [9], [10] first mixed CdSe/ZnS QD with polymethyl methacrylate (PMMA) to make an independent color conversion film which was also the concept of color filters. Thereafter, a blue OLED was utilized to excite a color conversion film and make white OLED. White OLED of this structure has a relatively high spectrum stability to resist the voltage variation. CIE coordinates are shifted only by (0.003, 0.001) from 4 to 8 V. And micro-pillar arrays are formed on the surface of QD color conversion films to improve the color deviation resulting from the angle of view and enhance the light extraction efficiency. By Hyo-Jun Kim *et al.*, red QDs were evenly dispersed in photoresist to form the QD photoresist film (PR film) which was pasted on the surface of WOLED. The red luminance intensity was improved with the help of QD color conversion [11], [12]. By Hyo-Jun Kim *et al.*, red and green QD materials were mixed with PGMEA and dispersed in positive photoresist. A photolithography process was carried out for the QD PR on the glass substrate, then a full-color OLED display was fabricated. Compared with traditional OLED displays, the luminance intensity of red and green sub-pixels has been improved by 32.1% and 9.6% respectively after the use of QD [13].

The use of blue OLED to excite QD color conversion film has gradually become a trend. In 2020, Zhiping Hu *et al.* published a paper in Nanoscale, concerning the application of QD color conversion film in OLED. They utilized blue OLED to excite red and green QD CCL. Firstly, they studied the methods to prepare the QD CCL solution. Two kinds of QD ink were prepared respectively. One was a volatile solvent (cyclohexylbenzene) and the other was a UV photo-curable polymer solvent (ingredients including acrylic resin, photoinitiator, cross-linking agent, etc.). The UV photo-curable QD polymer is involved in a polymerization reaction using UV light, and thus, the coffee rings will not be easily generated after curing. As a result, micron-level thick QD film with even surface morphology can be obtained, and high-efficiency color conversion efficiency can be realized. Additionally, the thickness of the QD layer can be varied to adjust the light conversion efficiency [13]. Zhiping Hu *et al.* [14] combined blue OLED with red and green QDs. High efficient full-color OLED displays are implemented. The CCL is coated with a polymer-based QD ink by ink-jet printing directly onto color filters. The light conversion efficiency (LCE) of the 10.2 μm green QD layer is 90% while that of the 10.5 μm red QD layer is 33%. QD CCL has effectively expanded the color gamut of OLED and improved luminance. Also many scholars directly utilized green and red luminous QD materials as the emitting layers in OLED to directly fabricate a white-light device [15]–[18].

II. Experiments

In this research, the PET/Indium Tin Oxide (ITO) flexible substrate (purchased from Ruilong Optoelectronics Co., Ltd. Taiwan) with a resistance of 40 Ω/sq and substrate thickness of 0.125 mm is employed. A laser engraving machine is utilized to define the patterns needed by the device. The emitting area is 1.0 cm $\times$ 1.0 cm. The substrate was immersed in acetone, isopropanol, and deionized water in sequence and washed with ultrasonic vibration for 20 minutes each. Thereafter, the substrate was blown dry with nitrogen (N_2) gun and then put into an oven for 10 minutes to bake at temperature of 80 °C. The organic layers were deposited by thermal vacuum evaporation system (at a vacuum pressure of 6×10^{-6} torr). The organic layers evaporated on the PET/ITO in the following order: the hole injection layer HATCN/hole transport layer TAPC/emitting layer MADN doped with ν-DABNA/ electron transport and hole blocking layer TPBi. Where ν-DABNA is N_7,N_7,N_{13},N_{13},5,9,11,15-octaphenyl-5,9,11,15-tetrahydro-5,9,11,15-tetraaza-19*b*,20*b*-diboradinaphtho[3,2,1-*de*:1′,2′,3′-*jk*]pentacene-7,13-diamine. Next, the substrate was transferred to the metal evaporation system. The LiF and Al was evaporated onto organic layer at vacuum of 8×10^{-6} torr. The deposition

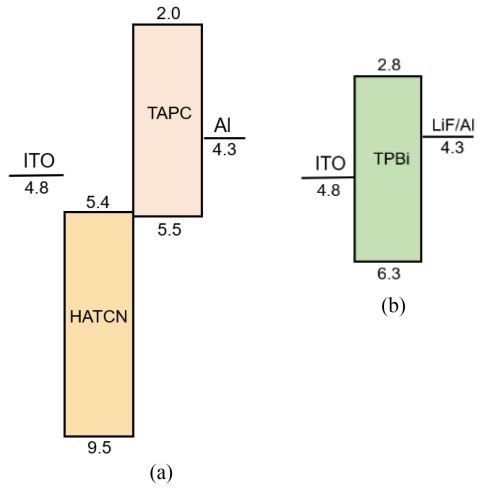

Fig. 1. Energy band diagram (a) hole only device and (b) electron only device.

rate and thickness of LiF are 0.1 Å/s and 0.8 nm respectively, while those of Al are 10 Å/s and 150 nm respectively. Thereafter, the fabrication of blue OLED was completed.

The CdSe/ZnS based QD photoresist (purchased from Yeh-Ji Industrial Co., Ltd. Taiwan) was spin-coated on glass or flexible substrates. The QD PR area relatively facing to the blue OLED emitting area was defined using adhesive tape. The spin-coating speeds of QD PR for different device structures were 600, 800, and 900 rpm, respectively, over 60 s each, and then put on a hot plate for 2 minutes to pre-bake at temperature of 80°C. After completion of the pre-baking, the SUSS MicroTec Mask Aligner was employed to expose and cure the QD PR for 50 seconds. Next, the substrate was placed on a hot plate to bake at temperature of 80 °C for 20 minutes to completely cure the QD PR CCL. Finally, the Keithley 2400 (power supply and current-voltage measurement) was used to provide a bias to the blue OLED and the Spectra Scan PR 650 Spectra Colorimeter was used to measure the luminance and spectra. The current-luminance-voltage (I-L-V) characteristic curves were obtained.

III. Results and Discussion

The HATCN is strongly oxidative and thus has a cleaning effect on the polluted ITO surface. The strong oxidant can also effectively withdraw electrons from an ITO surface (generating relatively more holes), thus, reducing the hole injection barrier to enhance the hole injection efficiency [1]–[3]. Since PET substrate is relatively unsuitable to be cleaned using organic solvents like acetone, HATCN is selected as the hole injection material. This study first explores whether the hole current in the blue OLED fabricated on PET/ITO (40 ohm/□) is balanced with the electron current. Therefore, PET/ITO/HATCN(10-15 nm)/TAPC(30 nm)/Al(150 nm) is utilized as a hole-only device. The energy band diagram and device parameters are shown in Fig. 1(a) and Table I, respectively. This structure has no evaporated LiF layer between TAPC and Al cathode, therefore the quantity of electron injections from cathode side is extremely low. Therefore, the hole current is the main current. Besides, PET/ITO/TPBi(20-30 nm)/LiF(0.8 nm)/Al (150 nm) is utilized

TABLE I
Device Parameters For Hole Only and Electron Only Devices
(unit: nm)

NO	HIL	HTL	ETL	EIL	Cathode
	HATCN	TAPC	TPBi	LiF	Al
HATCN-10	10	30	0	0	150
HATCN-15	15	30	0	0	
TPBi-20	0	0	20	0.8	
TPBi-30	0	0	30	0.8	

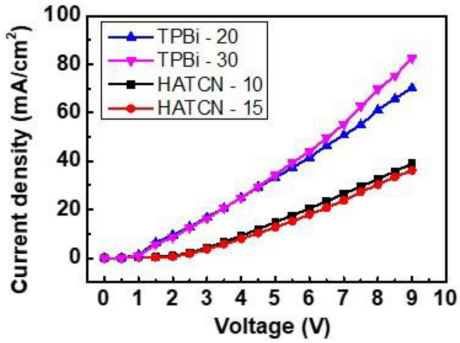

Fig. 2. Current density vs voltage for hole only and electron only devices.

to fabricate an electron-only device. The energy band diagram and device parameters are shown in Fig. 1(b) and Table I, respectively. The hole barrier of this structure between ITO work function and TPBi HOMO is as high as 1.5 eV. Therefore, the quantity of hole injections at the anode side is extremely low. Furthermore, the electron current from cathode side is the main current. The current density-voltage (J-V) characteristics of hole-only and electron-only devices are compared and shown in Fig. 2. It is found that the hole-only current is smaller than the electron-only current, possibly because the resistance value of ITO film is relatively high (40 ohm/□), thus, naturally resulting in smaller hole current. The effective resistance of the hole-only device can be calculated by the slope of current density-voltage (J-V) curve as 180-199 ohm (between 3-7 V). Then, it can be found from the energy band diagram shown in Fig. 1(a) that an energy barrier still exists between ITO work function and HATCN/TAPC. Therefore, the cut-in voltage is relatively high (about 2 V). As seen from the comparison in Fig. 2, the electron current of the electron-only device is relatively higher than hole-only current. The resistance of the electron-only device can be calculated by the slope of the J-V curve as approximately 114-126 ohm (between 2-5.5 V) and the cut-in voltage is about 1 V. It is clear that the electron injection barrier of TPBi/LiF/Al is lower than the hole injection barrier of ITO/HATCN/TAPC and has a relatively smaller effective resistance.

Also as seen from Fig. 2 in the electron-only device, when the thickness of TPBi is increased (from 20 to 30 nm), the electron transport amount is increased at high voltage. Therefore, the electron current is slightly increased. When the voltage is 9 V, the current density is increased from 70.25 to 82.46 mA/cm^2. In the hole-only device, the hole current of HATCN 15 nm is slightly lower than that of HATCN 10 nm.

The blue emitting materials used in this research are mainly MADN: 10 wt% ν-DABNA series [5]–[7]. The spectrum main

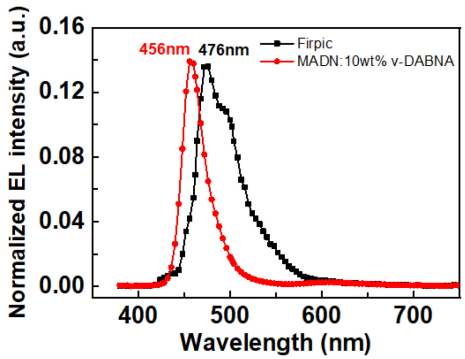

Fig. 3. EL spectra of blue OLED with EML of MADN:10% ν-DABNA and FIrpic.

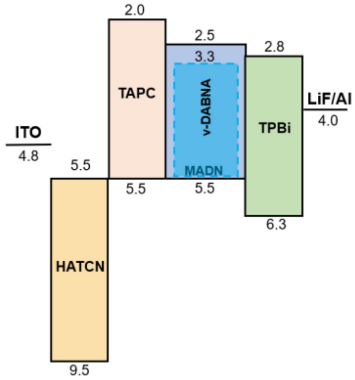

Fig. 4. Energy band diagram of blue OLED.

TABLE II
DEVICE PARAMETERS OF BLUE OLEDS WITH DIFFERENT TAPC (HTL) THICKNESSES

No.	HIL	HTL	EML	ETL
	HATCN	TAPC	MADN:10wt% ν-DABNA	TPBi
TAPC-20	10	20	50	30
TAPC-25		25		
TAPC-30		30		

peak is 456 nm with FWHM of 26 nm. Compared with Flrpic [19], the wavelength is shorter and the FWHM is narrower (FWHM 54 nm for FIrpic). It is a kind of purer blue light. The comparison of spectra of the aforementioned two is shown in Fig. 3. The CIE coordinates of ν-DABNA blue OLED is at (0.14, 0.08).

The thickness of the hole transport layer (HTL) TAPC is adjusted and changed to 20, 25, and 30 nm respectively in this section. Thereafter, the influence of the thickness of HTL on the device's characteristics is studied. The device structure is PET/ ITO/HATCN(10 nm)/TAPC(x nm)/MADN: 10 wt% v- DABNA(50 nm)/TPBi(30 nm)/LiF(0.8 nm)/Al(150 nm). The energy band diagram and device parameters are shown in Fig. 4 and Table II, respectively. Fig. 5(a), (b) and (c) show the current density-voltage (J-V), luminance-voltage (L-V), and yield-voltage (Y-V) characteristics curves of different TPAC thicknesses, respectively. Fig. 6 shows the emitting photograph of the flexible blue OLED. The research findings indicated in Fig. 2

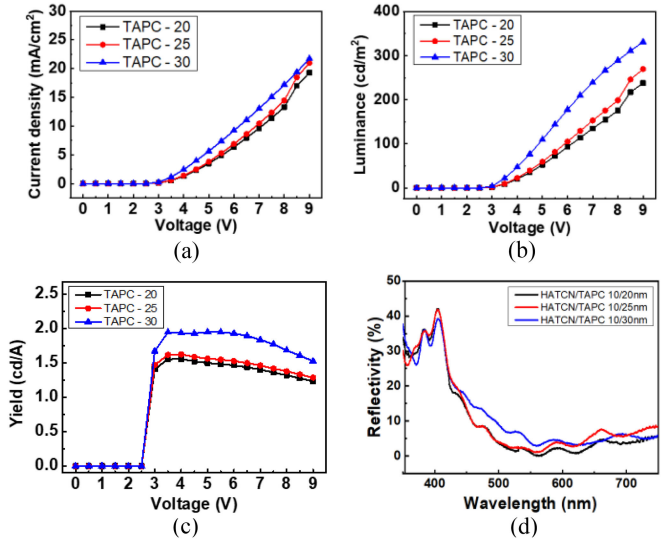

Fig. 5. Comparisons of (a) J-V, (b) L-V, (c) Y-V curves, and (d) Reflectance spectra of blue OLEDs with different TAPC thickness.

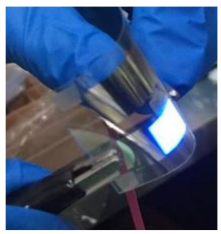

Fig. 6. The photo of light emitting of flexible blue OLED.

show that the hole injection current of PET/ITO/HATCN/TAPC (anode side) is lower than the electron injection current of TPBi/LiF/Al (cathode side). Therefore, the hole current must be increased to improve the luminance and efficiency. Compared with TAPC 30 nm, when TAPC thickness is 20 nm and 25 nm, the hole transport efficiency is relatively worse due to insufficient thickness, and the total current is relatively lower. When TAPC thickness is increased to 30 nm, the total current is increased. It is thus speculated that the hole current is increased with an increase of TAPC thickness as shown in Fig. 5(a). The increase of hole current results in the increase of electron-hole recombination amount. Therefore, the luminance and efficiency are improved as well, as shown in Fig. 5(b) and (c), respectively.

Saikia *et al.* used Bphen as the ETL to study the effect of different ETL thicknesses on the current-voltage characteristics of OLEDs. It is found that when the thickness of Bphen increases from 5 to 15 nm, the current density increases with the thickness. It is predicted that the function of Bphen to transport electrons and transport holes is just the opposite, and the increase in thickness of Bphen may block more holes, but help more electrons to conduct [20]. In this study, the HATCN/TAPC interface may have similar phenomena. The function of the HATCN/TAPC interface is like a charge generation layer (CGL). The LUMO energy level (low lying) of HATCN is very close to the HOMO energy level of TAPC, and the energy level difference between the two is very small. Therefore, electrons can be transferred

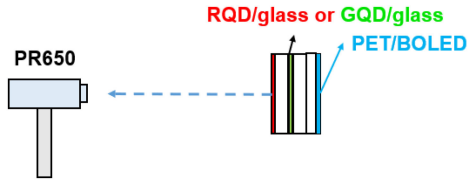

Fig. 7. The blue OLED and green and red QD CCLs are assembled to measure the spectra.

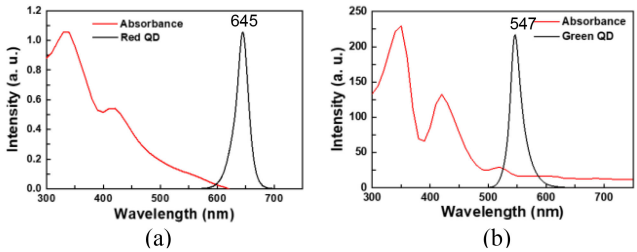

Fig. 8. Absorption and PL spectra of (a) red and (b) green QD PR.

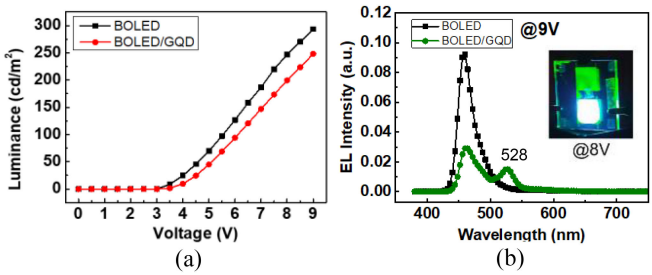

Fig. 9. (a) L-V curves of the color conversion of GQDs excited by the blue OLED, (b) spectra of GQD CCL excited by blue OLED at 9 V. The inserted photo: upper and lower pixels show the non-excited and excited GQD CCL by blue OLED, respectively.

from the HOMO energy level of TAPC to the LUMO energy level of HATCN, while the left holes in TAPC can be drifted to the EML, thus enhancing the hole injection efficiency [21].

Regarding 30 nm TAPC current density is larger than 20-25 nm (30 nm TAPC has lower bias at constant current), there may be two reasons. Reason (1): When the TAPC is thicker, more electrons can be transferred to the HATCN, thereby generating more holes to be injected into the EML. Reason (2): From the comparison of hole only current with electron only current in Fig. 2, it can be understood that the hole current of the blue OLED structure in this study is relatively lower. When a voltage is applied between the cathode and the anode, a partial voltage will be distributed between each layer. The thickness of 30 nm TAPC is thicker than that of 20-25 nm, so the 30 nm TAPC will be distributed with a higher partial voltage, prompting more holes drifted from HATCN to TAPC and then to the EML. Thus the hole current density increases and the total current density increases.

The increment of the luminance in this case may be ascribed to the increasing thickness which can help to enhance the light out coupling efficiency. The reflectance spectra of PET/ITO/HATCN/TAPC/MADN/TPBi samples with different TAPC thicknesses were measured as shown in Fig. 5(d). The reflectivity (R) at peak 456 nm for TAPC thickness of 20, 25 and 30 nm is 10.7, 11.1 and 14.9%, respectively. For the sample with 30 nm TAPC the reflectivity of 14.9% at 456 nm was higher than those samples with 20 and 25 nm TAPC, and higher reflectivity suggested lower light transmission, which help to exclude the possibility of higher light output coupling with 30 nm TAPC. Thus the reflectance spectra can only manifest that the higher luminance of sample with 30 nm TAPC may primarily be ascribed to the increase of hole current which results in the increase of electron-hole recombination amount. Therefore, the luminance and efficiency are improved as well.

In this research, the photoresist (PR) mixed with QD material is used as a color conversion layer (CCL) [12]. QD PR is coated on another piece of glass substrate and the aforesaid blue OLED is utilized to excite green and red QD CCL. The blue OLED and QD CCL are assembled to fabricate a white lighting panel. To study the characteristics of QD PR materials, the QD PR is coated on another piece of glass substrate for measurements first, as shown in Fig. 7, i.e., CCL remote excitation by blue OLED. The CCL used in this research is CdSe/ZnS-based QDs which are dispersed in photoresist. The absorption and fluorescence spectra of green QD (GQD) PR and red QD (RQD) PR are shown in Fig. 8(a) and (b), respectively. The quantum efficiency of green and red QD PR is 18% and 24%, respectively.

The thickness of GQD with 900 rpm spin-coated on glass is approximately 9.75 μm (by SEM cross section measurement) and is excited by the blue OLED. The luminance-voltage characteristics of the GQD CCL excited by the blue OLED are shown in Fig. 9(a). The spectra of GQD excited by blue OLED at 9 V is shown in Fig. 9(b). When the voltage is 9 V, luminance is 248.1 cd/m^2 and efficiency is 1.30 cd/A. The upper and lower pixels in the photo inserted in Fig. 9(b) show the non-excited and excited GQD CCL emission by blue OLED, respectively.

In this section, the blue OLED is used to excite the red quantum dots (RQD) CCL with different thicknesses. The relationship between RQD CCL thickness and red spectrum intensity excited is explored to acquire sufficient red emission intensity. The RQD CCL thickness obtained through the spin-coating speed of 600, 800, and 900 rpm is 14.2, 11.2, and 9.7 μm respectively. The lower the revolving speed, the thicker the RQD CCL. A relatively thick RQD CCL absorbs relatively abundant blue light to generate relatively strong red light (wavelength: 620 nm, FWHM: 30 nm), as shown in Fig. 10(a). For RQD CCL thickness of 11.2 and 14.2 μm, the peak intensity of excited red spectrum (620 nm) becomes higher than that of emitting blue spectrum (456 nm) from blue OLED. But when the RQD CCL thickness is relatively thinner as 9.75 μm, most of the blue light penetrates RQD CCL, and only a little red light is excited. Therefore, the red peak intensity is relatively weak. Fig. 10(b) indicates the CIE coordinates of RQD CCL with a spinning of 600, 800, and 900 rpm excited by 9 V blue OLED are (0.48, 0.28), (0.42, 0.25), and (0.32, 0.21) respectively. The 900 rpm spin-coated RQD CCL has a relatively thinner thickness of 9.75 μm and therefore the excited spectrum is blue light dominant. The 14.2 μm thick RQD CCL excited by blue OLED biased

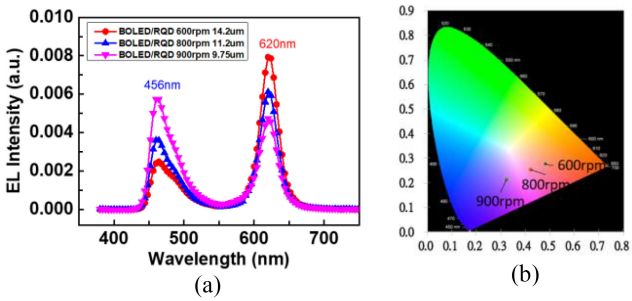

Fig. 10. (a) Spectra and (b) shift of CIE coordinates of RQD CCL with different spin-coating speeds and excited by blue OLED.

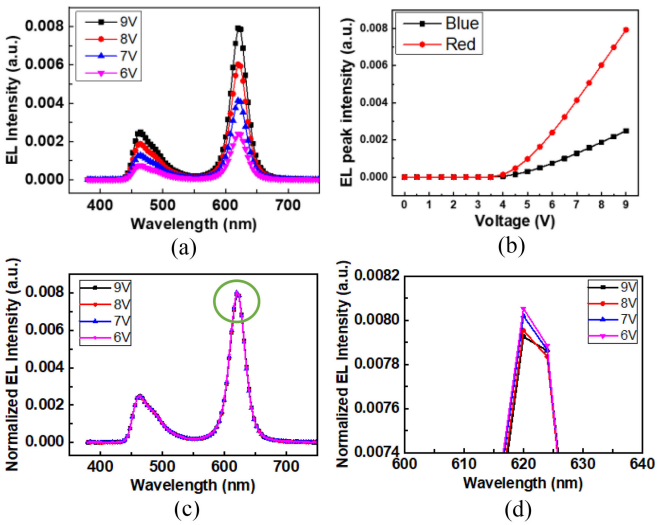

Fig. 11. (a) Spectra, (b) EL peak intensity of RQD CCL excited by blue OLED at various voltages, (c) normalized EL spectra with respective to the blue peak and (d) enlarged red peaks from (c).

at different voltages are studied. The red peak intensity of RQD CCL excited by blue OLED will increase and the blue peak itself slightly increase with applied voltage of blue OLED, and their spectral comparison is shown in Fig. 11(a). The comparison of the peak intensity of blue and red spectra is shown in Fig. 11(b). It is clear that the color conversion efficiency is relatively high when the thickness of RQD CCL is thick enough. When the thickness of RQD CCL is 9.75 μm, the thickness is insufficient, resulting in the blue light absorption not enough. Most of the blue light penetrates and therefore the color conversion cannot realize the expected efficiency. In order to study the EL spectral stability, the EL spectra of Fig. 11(a) are normalized for RQD CCL-based OLEDs as shown in Fig. 11(c), where the blue peak intensity is employed as reference intensity. After normalization, the EL spectra look very stable for RQD+OLEDs biased at different voltages. So the red peak from Fig. 11(c) is enlarged and shown in Fig. 11(d).

Finally, GQD photoresist and RQD photoresist are mixed with a proper ratio (GRQD) and then directly spin-coated on the back of a PET/ITO substrate as a color conversion layer. Thereafter, the blue OLED processes were carried out on ITO surface. This kind of structure makes the light emitted from

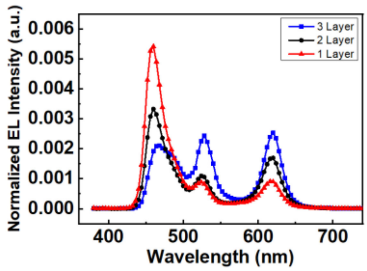

Fig. 12. The excitation spectra from GRQD CCL with spin- coating of 1 layer, 2 layers, and 3 layers, respectively, excited by blue OLED.

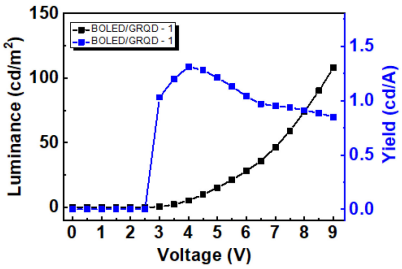

Fig. 13. L-V and Y-V curves of the GRQD CCLs/PET/ITO /blue OLED assembled devices.

blue OLED directly excite the GRQD CCL to mix red, green, and blue color to generate the white light. This structure can also improve color conversion efficiency and avoid causing too much waveguide loss like remote excitation structure. The thickness of the GRQD CCL is an important parameter. The excitation spectra obtained from GRQD CCL with spin-coating of 1 layer, 2 layers, and 3 layers, respectively, are shown in Fig. 12. For 1 layer of GRQD CCL, the experimental parameters are spin-coating: 600 rpm/40 sec, pre-baking: 80 °C/60 sec, UV exposure: 50 sec, post-baking 80 °C/15 min. The experimental procedure was repeated 2 and 3 times for 2 and 3 layers, respectively. The thickness of 1, 2 and 3 layers of GRQD CCL is about 7.3, 12.0 and 17.2 μm, respectively, by SEM cross section measurement. For spin-coating of one and two layers of GRQD CCL, the green and red peak intensity are much weaker than that of blue light, so the white light cannot be formed.

The excited green and red peak intensity will not be stronger than that of blue light and white light cannot be formed until three layers of GRQD CCLs are spin-coated. The luminance-voltage and efficiency-voltage characteristics of the GRQD CCLs/PET/ITO/blue OLED assembled devices are shown in Fig. 13. The luminance and efficiency are 108 cd/m^2 and 0.85 cd/A at 9 V, respectively. The maximum efficiency is 1.3 cd/A @ 4 V. The white EL spectra from 6 to 9 V are successfully obtained, as shown in Fig. 14(a), by GRQD CCL directly spin-coated on the back of blue OLED substrate. The white EL spectra have three peaks which are 456, 528 and 620 nm, respectively. The CIE coordinates from 6 to 9 V are quite stable at (0.35, 0.35), as shown in Fig. 14(b), and independent with the applied voltage. The white lighting panel is successfully obtained by simply processes. In order to study the EL spectral

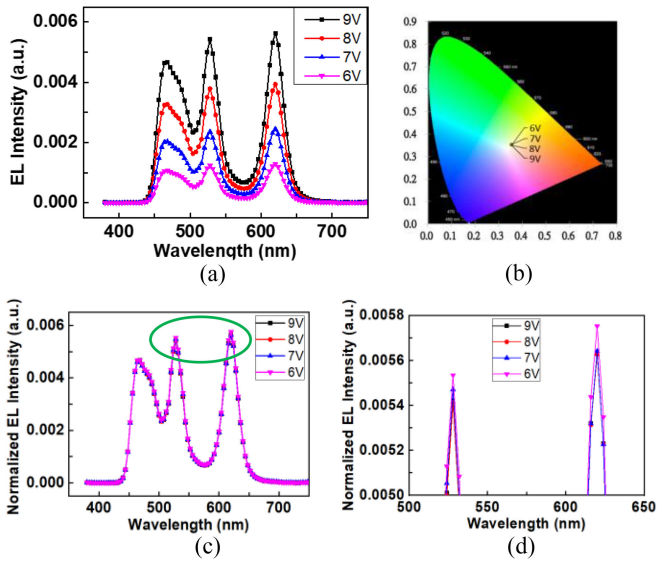

Fig. 14. (a) White EL spectra and (b) CIE coordinates from 6 to 9 V by GRQD CCL directly spin-coated on the back of blue OLED. (c) Normalized EL spectra with respective to the blue peak and (d) enlarged green and red peaks from (c).

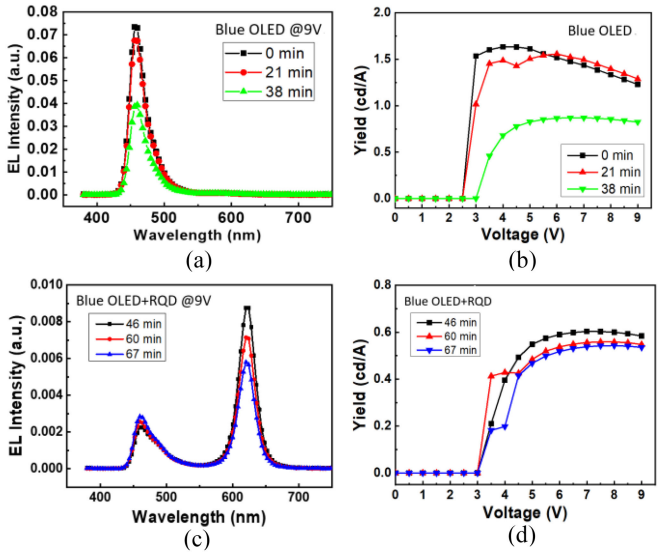

Fig. 15. (a) EL spectra of blue OLED @9V and (b) current efficiency vs voltage of blue OLED measured at different times. (c) EL spectra of RQD+blue OLED @9V and (b) current efficiency vs voltage of RQD+blue OLED measured at different times.

stability, the EL spectra of Fig. 14(a) are normalized for GRQD CCL-based OLEDs as shown in Fig. 14(c), where the blue peak intensity is employed as reference intensity. After normalization, the EL spectra look very stable for GRQD+OLEDs biased at different voltages. So the green and red peaks from Fig. 14(c) are enlarged and shown in Fig. 14(d).

Finally the time-dependent efficiency and spectral stability of blue OLED and RQD excited by blue OLED without encapsulations were examined. The EL blue peak intensity and current efficiency of pure blue OLED @9V decreased from 0.073 to 0.039 a.u. and from 1.23 to 0.82 cd/A after 38 min, as shown in Fig. 15(a) and (b), respectively. The EL red peak intensity of RQD excited by blue OLED @9V decreased from 0.021 to 0.0058 a.u. after 67 min, as shown in Fig. 15(c). Its current efficiency decreased from 1.23 to 0.54 cd/A after 67 min as shown in Fig. 15(d). In the future the thin-film encapsulation method for flexible OLED+QD lighting will be studied to extend the lifetime.

IV. Conclusion

In this study, the HATCN is deposited on flexible PET/ITO substrate as a modified and hole injection layer. Without O_2 plasma or UV Ozone treatment on ITO surface, the blue OLED is successfully fabricated with the structure of PET/ITO/HATCN(10 nm)/TAPC(30 nm)/MADN:10 wt% ν-DABNA (50 nm) /TPBi (30 nm)/LiF (0.8 nm)/Al(150 nm). The electron and hole current density are compared in electron-only and hole-only device, respectively. Since the resistance of PET/ITO is relatively high (40 ohm), the hole current at anode side in hole only device is 20 mA/cm^2 which is lower than the electron current at cathode side in electron only device of 40 mA/cm^2 at 6 V. A new TADF series fluorescent material ν-DABNA is adopted as blue emitting layer with luminescence wavelength of 456 nm and very narrow FWHM of 26 nm (FIrpic 40 nm). When the TAPC (HTL) thickness is adjusted to 30 nm, the optimum blue luminance and efficiency of 331.04 cd/m^2 and 1.52 cd/A at 9 V are obtained, respectively, for emitting area of 1 cm $\times$ 1 cm. The blue chromaticity is excellent. QD photoresist material is a perfect color conversion material with a high fluorescence efficiency and simple coating processes. In this research, photoresist mixed with green and red QDs is utilized as CCL, and blue OLED is utilized for excitation. At first, the green and red QD CCLs were remotely excited by blue OLED to acquire spectra of 528 and 620 nm, respectively. Finally, green and red QD photoresist is mixed with a proper ratio and then directly spin-coated on the back of a PET/ITO/blue OLED substrate. As seen from the experiments, the blue OLED can only excite the QD CCL with sufficient thickness to generate green and red spectra with sufficient intensity so as to form the white light. By adjusting the thickness of the QD CCL, the blue OLED directly excites QD CCL to generate three primary colors of blue, green and red (456, 528 and 620 nm). In this study, simple processes are employed to successfully fabricate a flexible white lighting panel with blue OLED and down-conversion QD CCL assembled. The CIE coordinates from 6 to 9 V are quite stable and fixed at (0.35, 0.35), independent with the applied voltage.

Acknowledgment

The authors thanks to Dr. Pei S. Yeh for materials and experimental supports. The authors thanks to Prof. Shu-Ru Chung, Department of Materials Science and Engineering, National Formosa University for absorption and PL measurement of QD materials. The authors thanks to Prof. Day-Shan Liu, Department of Electro-Optical Engineering, National Formosa University for UV-VIS measurement of OLED devices.

REFERENCES

[1] X. Tang, M. Qian, D. Y. Zhou, and L. Ding, "A surface modification layer capable of tolerating substrate contamination on transparent electrodes of organic electronic devices," *Org. Electron.*, vol. 28, pp. 217–224, 2016.

[2] H. Kang, J. H. Kim, J. K. Kim, J. Seo, and Y. Park, "Interface electronic structure of a strongly electron withdrawing molecule on an indium-tin-oxide surface," *J. Korean Phys. Soc.*, vol. 59, pp. 3060–3063, 2011.

[3] Z. L Yang, C. Cheng, X. D. Pan, F. Pan, F. Wang, and M. Y. Tian, "Effects of hole injection layer on performance of green OLEDs based on flexible ITO," *Mater. Chem. Phys.*, vol. 239, 2020, Art. no. 121828.

[4] D. Dong *et al.*, "Enhanced hole injection by introducing an electron-withdrawing layer in inverted quantum dot light-emitting diodes," *Org. Electron.*, vol. 68, pp. 22–27, 2019.

[5] T. Hatakeyama and K. Shiren, "Ultrapure blue thermally activated delayed fluorescence molecules: Efficient HOMO–LUMO separation by the multiple resonance effect," *Adv. Mater.*, vol. 28, pp. 2777–2781, 2016.

[6] Y. Kondo *et al.*, "Narrowband deep-blue organic light-emitting diode featuring an organoboron-based emitter," *Nature Photon.*, vol. 13, pp. 678–682, 2019.

[7] S. O. Jeon *et al.*, "High-efficiency, long-lifetime deep-blue organic light-emitting diodes," *Nature Photon.*, vol. 15, pp. 208–215, Mar. 2021. [Online]. Available: https://doi.org/10.1038/s41566-021-00763-5

[8] C. Yoon *et al.*, "Highly luminescent and stable white light-emitting diodes created by direct incorporation of CD-free quantum dots in silicone resins using the thiol group," *J. Mater. Chem. C*, vol. 3, pp. 6908–6915, 2015.

[9] M. Yin, Z. Yu, T. Pan, X. Peng, X. Zhang, and L. Zhang, "Efficient and angle-stable white top-emitting organic light emitting devices with patterned quantum dots down-conversion films," *Org. Electron.*, vol. 56, pp. 46–50, 2018.

[10] M. Yin *et al.*, "Color-stable WRGB emission from blue OLEDs with quantum dots-based patterned down-conversion layer," *Org. Electron.*, vol. 62, pp. 407–411, 2018.

[11] H. J. Kim, M. H. Shin, J. Y. Lee, J. H. Kim, and Y. J. Kim, "Realization of 95% of the Rec. 2020 color gamut in a highly efficient LCD using a patterned quantum dot film," *Opt. Exp.*, vol. 25, pp. 10724–10734, 2017.

[12] H. J. Kim *et al.*, "Enhancement of optical efficiency in white OLED display using the patterned photoresist film dispersed with quantum dot nanocrystals," *J. Display Technol.*, vol. 12, pp. 526–531, 2016.

[13] H.-J. Kim, M.-H. Shin, J.-S. Kim, S.-E. Kim, and Y.-J. Kim, "High efficient OLED displays prepared with the air-gapped bridges on quantum dot patterns for optical recycling," *Sci. Rep.*, vol. 7, 2017, Art. no. 43063, doi: 10.1038/srep43063.

[14] Z. Hu *et al.*, "Inkjet printed uniform quantum dots as color conversion layers for full-color OLED displays," *Nanoscale*, vol. 12, pp. 2103–2110, 2019.

[15] L. A. Kim *et al.*, "Contact printing of quantum dot light-emitting devices," *Nano Lett.*, vol. 8, no. 12, pp. 4513–4517, 2008.

[16] S. Dai, C.-B. Siao, S.-R. Chung, K.-W. Wang, and X. Pan, "Developed one-pot synthesis of dual-color cdse quantum dots for white light-emitting diode application," *J. Mater. Chem. C*, vol. 6, pp. 3089–3396, 2018.

[17] C. Jiang *et al.*, "Fully solution-processed tandem white quantum-dot light emitting diode with an external quantum efficiency exceeding 25%," *ACS Appl. Mater. Interfaces*, vol. 12, no. 6, pp. 6040–6049, 2018.

[18] D. Dong, L. Lian, H. Wang, and G. He, "An efficient solution-processed hole injection layer with phosphomolybdic acid in quantum dot light-emitting diodes," *Org. Electron.*, vol. 62, pp. 320–326, 2018.

[19] J. Liu *et al.*, "High-efficient sky-blue and green emissive OLEDs based on FIrpic and FIrdfpic," *Synthetic Met.*, vol. 234, pp. 111–116, 2017.

[20] D. Saikia and R. Sarma, "Comparative study of OLED using various thickness of electron transport layer," *Indian J. Sci. Res.*, vol. 13, no. 1, pp. 99–103, 2017.

[21] R. Rana and R. Mehra, "Investigation of organic LED materials using a transparent cathode for improved efficiency," *J. Electron. Mater.*, vol. 48, no. 7, pp. 4409–4417, 2019. [Online]. Available: https://doi.org/10.1007/s11664-019-07221-7